Journal of Materials Chemistry A

Accepted Manuscript

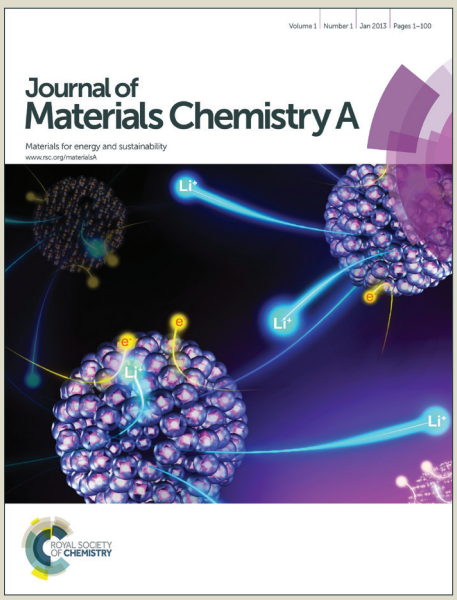

ROYAL SOCIETY OF CHEMISTRY

www.rsc.org/materialsA

Aligned carbon nanotube/molybdenum disulfide hybrids for effective fibrous supercapacitors and lithium ion batteries

Yongfeng Luo,[†ab] Ye Zhang,[†a] Yang Zhao,[a] Xin Fang,[a] Jing Ren,[a] Wei Weng, [a] Yishu Jiang, [a] Hao Sun, [a] Bingjie Wang, [a] Xunliang Cheng and Huisheng Peng*

[a]*State Key Laboratory of Molecular Engineering of Polymers, Department of Macromolecular Science, and Laboratory of Advanced Materials, Fudan University, Shanghai 200438, China; Email: penghs@fudan.edu.cn.*

[b]*College of Science, Central South University of Forestry and Technology, Changsha, Hunan 410004, China.*

[†]*These authors contributed equally to this work.*

Abstract: An aligned carbon nanotube/MoS_2 nanosheet hybrid fiber was synthesized to display combined remarkable mechanical, electronic and electrochemical properties. It was used to fabricate flexible fibrous supercapacitors and lithium ion batteries with high specific capacitance of 135 F cm^{-3} and high specific capacity of 1298 mAh g^{-1}, respectively.

Introduction

The wearable electronics industry is widely recognized to be undergoing a technological revolution, the efforts of which are currently being hindered by challenges in finding suitably wearable power systems. The planar and bulky structure in the conventional energy storage devices such as supercapacitors and lithium ion batteries (LIBs) cannot effectively meet the requirement to be flexible, integratable and weaveable[1-10]. To this end, a family of fibrous supercapacitors[10-14] and LIBs[15-17] was developed to solve this problem. However, the electrochemical performances are much lower than their planar counterparts due to the difficulty in finding appropriate fibrous electrodes that are expected to be flexible and strong with combined high electrical conductivity and electrochemical activity[18, 19].

The fibrous electrodes were extensively constructed from aligned carbon nanotube (CNT) fibers with both remarkable electrical and mechanical properties but with intrinsically limited energy storage capabilities[20]. Therefore, functional components like polyaniline,[21] MnO_2[22] and $LiMn_2O_4$[16] were incorporated to enhance the performance. The electrochemical performances of these composite electrodes were

strongly dependent on the interface between the CNT and guest component, which had an important impact on the electron transport and ion migration. CNT fibers can be hybridized with functional components through chemical and physical approaches. For instance, conducting polymers were deposited onto the surface of CNT fibers by electrochemical polymerization[2], while $LiMn_2O_4$ particles were embraced within CNT fibers through a solution-based deposition[16] . Although the effectiveness of these methods has been demonstrated, several problems still reside: first, the chemically deposited materials incline to adhere on the surface of CNT fiber and the inside is rarely accessed; second, the active materials that have been embraced in CNT fibers are weakly anchored on the CNT and are prone to agglomerate, leading to an incomplete utilization. Hence, the introduced guest components are less able to offer substantial advantages to fibrous electrodes.

Molybdenum disulfide (MoS_2) is a typical two-dimensional layered transition-metal dichalcogenide material. MoS_2 nanosheets show high energy storage capacity[23-25], which is widely appreciated as an alternative material in supercapacitors[26] and LIBs[4, 27-29]. However, due to the low conductivity of MoS_2, the high electrochemical properties cannot be effectively utilized. Besides, it is difficult to synthesize single or few-layered MoS_2 nanosheets which can provide the largest surface area and are extremely useful for energy storage[30, 31].

In this Communication, an aligned CNT/MoS_2 hybrid was synthesized with few-layered MoS_2 nanosheets wound on the surface of the CNT. Here, aligned CNTs were used as templates for confining and directing the growth of MoS_2 nanosheets to form a curved structure around them. The designed hybrid nanostructure efficiently combined the superiority of high electrical conductivity in CNT and high energy storage capacity in MoS_2, which was promising for energy storage. Both fibrous supercapacitors and LIBs were thus fabricated from the hybrid fibrous electrode to exhibit higher electrochemical performances compared with the previous planar and other fibrous counterparts[32-36]. For instance, the specific capacitance achieved 135 F cm^{-3} at 5 mV s^{-1} in the fibrous supercapacitor and the specific capacity reached 1298 mAh g^{-1} at 0.2 A g^{-1} in the fibrous LIB. Besides, both fibrous supercapacitors and LIBs were flexible and weaveable, which satisfied the next-generation wearable and portable electronics.

Experimental section

Synthesis of aligned CNT/MoS_2 hybrid nanostructure. Typically, 34.2 mg of poly (vinyl pyrrolidone) (M_w of 40000) was dissolved in 70 mL of *N,N*-dimethylformamide under vigorous stirring for 1 h. Afterwards, 137 mg of ammonium tetrathiomolybdate was

added to the resulting solution, followed by an ultrasonic treatment for 2 h and vigorous stirring for 10 h to produce a homogeneous precursor solution. The precursor solution was then transferred to a Teflon-lined stainless steel autoclave (100 mL). The aligned CNT sheets that had been paved on a polytetrafluoroethylene substrate were then immersed in the precursor solution. The autoclave was heated in a muffle furnace at 220 ℃ for 6 h. After cooled down to room temperature, the synthesized aligned CNT/MoS_2 hybrid sheet was twisted into a fiber, followed by drying at 80 ℃ for 12 h.

Fabrication of fibrous supercapacitors and LIBs. Two aligned CNT/MoS_2 hybrid fibers that served as electrodes were coated with a layer of gel electrolyte and twisted into a fibrous supercapacitor. The used gel electrolyte was prepared by dissolving 0.67 g of poly (vinyl alcohol) in 6.04 g of deionized water at 90 ^oC for 5 h, followed by addition of 0.67 g of H_3PO_4. For the fibrous LIB, an aligned CNT/MoS_2 hybrid fiber was used as the cathode and paired with a lithium wire anode. The ends of the two electrodes were connected to copper wires by silver glue for further electrochemical measurement. The two electrodes were sealed in a heat-shrinkable tube with a separator between them. $LiPF_6$ (1 M) in a solvent mixture of ethylene carbonate, diethyl carbonate and dimethyl carbonate (weight ratios of 1:1:1) was used as the electrolyte (also called LB303), which was injected into the tube at the final step. The fabrication of the fibrous LIB was carried out in an Ar-filled glove box (MIKROUNA Super 1220/750).

Results and discussion

The synthesis of aligned CNT/MoS_2 hybrid nanostructure is schematically illustrated in Fig. 1a. Aligned CNT sheets were dry-drawn from spinnable CNT arrays[37] (Fig. S1) and then immersed in a reaction solution containing $(NH_4)_2MoS_4$ as a MoS_2 precursor and polyvinylpyrrolidone as a surfactant. During the solvothermal synthesis, MoS_2 nanosheets were found to be prone to grow on the outer walls of individual CNTs due to their high surface energy. Each CNT was wrapped by a layer of MoS_2 nanosheets and MoS_2 nanosheets were then continually grown on the wrapped CNT to form an aligned hybrid nanostructure (Fig. S2 and S3). The energy dispersive X-ray spectroscopy further shows that the CNT were uniformly wrapped with MoS_2 (Fig. S4).

The above CNT/MoS_2 hybrid sheets were finally twisted into the hybrid fiber. The hybrid fiber showed a uniform diameter of ~65 μm (Fig. 1b). The MoS_2 nanosheets were well distributed, and the CNT remained highly aligned in the hybrid fiber (Fig. 1c and 1d). In other words, the MoS_2 nanosheets had been well wrapped on the aligned CNT. The high-magnification transmission electron microscopy (TEM) image showed that these aligned hybrid nanostructures were constructed from ultrathin MoS_2

nanosheets. The MoS_2 nanosheets adopted a fashion of intergrowth to support each other and interwove together into a hybrid nanostructure along the aligned CNT, preventing the aggregation of MoS_2 nanosheets (Fig. 1e). The Brunner-Emmet-Teller surface area of the hybrid fiber was calculated to be as high as 187.6 m^2/g from Nitrogen adsorption-desorption isotherms (Fig. S5). The selected-area electron diffraction pattern of the MoS_2 nanosheet revealed a typical polycrystalline structure (Fig. 1e), and it exhibited an interlayer spacing of 0.63 nm (Fig. 1f). X-ray photoelectron spectroscopy was used to investigate the chemical states of Mo and S (Fig. 1g). The binding energies of Mo $3d_{3/2}$, Mo $3d_{5/2}$ peaks are located at 231.8 and 228.6 eV, respectively, indicating the formation of Mo^{4+} in MoS_2. The binding energies of S $2p_{1/2}$ and S $2p_{3/2}$ are located at 163 and 161.6 eV, respectively, which were attributed to the S^{2-} of MoS_2.[38, 39]

The interaction between CNT and MoS_2 in the hybrid fiber had been analyzed by Raman spectroscopy (Fig. S6). The G band of the CNT in the aligned CNT/MoS_2 hybrid fiber was located at 1587.5 cm^{-1}.[40] Compared with the bare CNT fiber, the G band of the CNT exhibited a red-shift of 6 cm^{-1} due to the change in the electronic structure of CNT after wrapped with MoS_2 nanosheet.[31] On the other hand, the MoS_2 nanosheet was well wrapped on the curved CNT even after the hybrid fiber was bent for 1000 cycles, which also verified the strong interaction between MoS_2 nanosheet and CNT (Fig. S7). The resistances were further traced during the bending cycles to verify the structural integrity of the hybrid fiber (Fig. S8). The resistances were varied in less than 1% after bending for hundreds of cycles.

To fabricate a fibrous supercapacitor, two hybrid fibers were first coated with a layer of poly (vinyl alcohol)/H_3PO_4 gel electrolyte and then twisted together. The gel electrolyte also functioned as the diaphragm to prevent short circuit. The structure of the fibrous supercapacitor is schematically illustrated in Fig. 2a and the electrochemical performance was carefully tested. The cyclic voltammograms exhibited a typical rectangular shape, indicating an electrical double-layer behavior (Fig. 2b). In addition, the rectangular shape had been well maintained with increasing scan rates from 5 to 100 mV s^{-1}. A high specific capacitance of 135 F cm^{-3} was achieved at the scan rate of 5 mV s^{-1} and was slightly decreased with the increasing scan rate (Fig. 2c). The high stability reflected by the cyclic voltammetry was also verified by the galvanostatic charge-discharge profiles that maintained a triangular shape at increasing current densities from 1 to 10 A cm^{-3} (Fig. 2d). According to the discharge curves, the specific capacitance can be maintained by 92% after 10000 charge-discharge cycles (Fig. 2e). The high rate performance and cyclic property may be explained by the effective interaction between MoS_2 nanosheet and CNT in the hybrid fiber.

The fibrous supercapacitor exhibits power densities up to ~0.55 W cm^{-3} and energy densities up to ~3 mWh cm^{-3}, which outperform the commercially available supercapacitor (5.5V/100 mF)[3] and other flexible supercapacitors (Fig. 2f).[32, 33] The high performance of the CNT/MoS_2 fiber electrode is explained below. The aligned CNT fiber not only acts as a freestanding physical support but effectively functions as a conductive pathway for the rapid transport of electrons. The MoS_2 nanosheets offer high specific surface areas for charge absorption and provide large contact areas for electrolyte. Apart from the high electrochemical performances, the CNT/MoS_2 hybrid fiber also contributed to high flexibility and deformation stability (Fig. S9). As shown in Fig. 2g-2i, the galvanostatic charge-discharge curves at increasing bending angles were perfectly overlapped and the specific capacitances were well maintained after bending into different angles. Moreover, after 1000 times of repeated bending deformations, the specific capacitance had been maintained by 95%.

Given that MoS_2 has the capability of storing lithium, the CNT/MoS_2 hybrid fiber can also serve as a fibrous cathode to produce fibrous LIBs. An aligned CNT/MoS_2 hybrid fiber and a lithium wires were assembled to fabricate a fibrous LIB (Fig. 3a). The first three charge-discharge curves at 0.2 A g^{-1} are shown in Fig. 3b. The plateaus from the charge-discharge curves agreed with the peaks observed in the cyclic voltammograms (Fig. 3c). The fibrous LIB showed a high cycling performance, and the specific capacity was maintained above 1250 mAh g^{-1} after 100 charge and discharge cycles (Fig. 3d). The specific capacity was calculated from the charge and discharge curves according to $C=I\times t/m$, where I, t and m correspond to the current, discharge time and mass of the cathode, respectively. Here the specific capacity was calculated from the whole electrode. The high value was derived from the high weight percentage of MoS_2 (e.g., 86%) in the hybrid fiber electrode besides the fact that no metal current collector, binder and conductive agent were used.

The CNT/MoS_2 cathode also exhibited a good rate performance (Fig. 3e). The specific capacity reached 1084 mAh g^{-1} at 0.5 A g^{-1}, 966 mAh g^{-1} at 1 A g^{-1} and 720 mAh g^{-1} at 2 A g^{-1}. Fig. 3f further compares the capacity of the present LIB with the reported planar MoS_2-based LIBs, and it exceeded the previous reports[34-36]. We can conclude the CNT/MoS_2 fiber electrodes have several advantages: it is not necessary to use conductive agent or metal current collector; the few layers of MoS_2 nanosheets decrease the transport distance of lithium ions, which further increases the rate of lithium insertion and deinsertion; the channels among MoS_2 nanosheet-wrapped CNTs are propitious to the infiltration of the electrolyte. The strong interaction between the MoS_2 nanosheet and CNT makes the hybrid fiber sustainable to various deformations without sacrificing performances. Similar to the fibrous supercapacitor, the fibrous LIB was

also flexible and can stably work under bending and after bending for over hundreds of cycles (Fig. 3g–3i).

Conclusion

In conclusion, a novel aligned CNT/MoS_2 hybrid nanostructure has been prepared to effectively combine the advantages of CNT and MoS_2 with remarkable electrochemical performances. Both fibrous supercapacitors and LIBs are further developed from these hybrid fibers and display much higher energy storage capacities than the previous planar and fibrous counterparts. These fibrous energy storage devices are flexible and weaveable and show promising applications in the next-generation wearable and portable electronics. This work also presents a general and effective paradigm in developing high-performance electrodes for efficient electronic devices.

Acknowledgements

This work was supported by NSFC (21225417), MOST (2011CB932503), STCSM (12nm0503200), Fok Ying Tong Education Foundation, the Program for Professor of Special Appointment at Shanghai Institutions of Higher Learning, and the Program for Outstanding Young Scholars from Organization Department of the CPC Central Committee.

Reference

1. J. Ren, L. Li, C. Chen, X. Chen, Z. Cai, L. Qiu, Y. Wang, X. Zhu and H. Peng, *Adv. Mater.*, 2013, **25**, 1155-1159.
2. Z. Cai, L. Li, J. Ren, L. Qiu, H. Lin and H. Peng, *J. Mater. Chem. A*, 2012, **1**, 258-261.
3. D. Yu, K. Goh, H. Wang, L. Wei, W. Jiang, Q. Zhang, L. Dai and Y. Chen, *Nat. Nanotechnol.*, 2014, **9**, 555-562.
4. G. Sun, X. Zhang, R. Lin, J. Yang, H. Zhang and P. Chen, *Angew. Chem.*, 2015, **127**, 4734-4739.
5. L. Kou, T. Huang, B. Zheng, Y. Han, X. Zhao, K. Gopalsamy, H. Sun and C. Gao, *Nat. Commun.*, 2014, **5**, 3754..
6. Y. Meng, Y. Zhao, C. Hu, H. Cheng, Y. Hu, Z. Zhang, G. Shi and L. Qu, *Adv. Mater.*, 2013, **25**, 2326-2331.

7. H. Chen, S. Zeng, M. Chen, Y. Zhang and Q. Li, *Carbon*, 2015, **92**, 271-296.
8. J. Zhong, Y. Zhang, Q. Zhong, Q. Hu, B. Hu, Z. L. Wang and J. Zhou, *ACS Nano*, 2014, **8**, 6273-6280.
9. X. Wang, X. Lu, B. Liu, D. Chen, Y. Tong and G. Shen, *Adv. Mater.*, 2014, **26**, 4763-4782.
10. W. Lu, M. Zu, J. H. Byun, B. S. Kim and T. W. Chou, *Adv. Mater.*, 2012, **24**, 1805-1833.
11. Z. Yang, J. Deng, X. Chen, J. Ren and H. Peng, *Angew. Chem. Int. Ed.*, 2013, **52**, 13453-13457.
12. V. T. Le, H. Kim, A. Ghosh, J. Kim, J. Chang, Q. A. Vu, D. T. Pham, J.-H. Lee, S.-W. Kim and Y. H. Lee, *ACS Nano*, 2013, **7**, 5940-5947.
13. P. Xu, T. Gu, Z. Cao, B. Wei, J. Yu, F. Li, J. H. Byun, W. Lu, Q. Li and T. W. Chou, *Adv. Energy Mater.*, 2014, **4**, 1300759.
14. Y. Fu, X. Cai, H. Wu, Z. Lv, S. Hou, M. Peng, X. Yu and D. Zou, *Adv. Mater.*, 2012, **24**, 5713-5718.
15. Y. Zhang, W. Bai, J. Ren, W. Weng, H. Lin, Z. Zhang and H. Peng, *J. Mater. Chem. A*, 2014, **2**, 11054-11059.
16. J. Ren, Y. Zhang, W. Bai, X. Chen, Z. Zhang, X. Fang, W. Weng, Y. Wang and H. Peng, *Angew. Chem.*, 2014, **126**, 7998-8003.
17. W. Weng, Q. Sun, Y. Zhang, H. Lin, J. Ren, X. Lu, M. Wang and H. Peng, *Nano Lett.*, 2014, **14**, 3432-3438.
18. K. Torchała, K. Kierzek, G. Gryglewicz and J. Machnikowski, *Electrochim. Acta*, 2015, **167**, 348-356.
19. M. Jin, G. Han, Y. Chang, H. Zhao and H. Zhang, *Electrochim. Acta*, 2011, **56**, 9838-9845.
20. R. H. Baughman, A. A. Zakhidov and W. A. De Heer, *Science*, 2002, **297**, 787-792.
21. Z. B. Cai, L. Li, J. Ren, L. B. Qiu, H. J. Lin and H. S. Peng, *J.Mater. Chem. A*, 2013, **1**, 258-261.
22. C. Choi, J. A. Lee, A. Y. Choi, Y. T. Kim, X. Lepró, M. D. Lima, R. H. Baughman and S. J. Kim, *Adv. Mater.*, 2014, **26**, 2059-2065.
23. T. Stephenson, Z. Li, B. Olsen and D. Mitlin, *Energy Environ. Sci* ., 2014, **7**, 209-231.
24. C. H. Lai, M. Y. Lu and L. J. Chen, *J. Mater. Chem.*, 2012, **22**, 19-30.
25. S. Zhang and N. Pan, *Adv. Energy Mater.*, 2015, **5**. DOI: 10.1002/aenm.201401401.

26. E. G. da Silveira Firmiano, A. C. Rabelo, C. J. Dalmaschio, A. N. Pinheiro, E. C. Pereira, W. H. Schreiner and E. R. Leite, *Adv. Energy Mater.*, 2014, **4**, 1301380.
27. C. Zhu, X. Mu, P. A. van Aken, Y. Yu and J. Maier, *Angew. Chem. Int. Ed.*, 2014, **53**, 2152-2156.
28. F. Zhou, S. Xin, H. W. Liang, L. T. Song and S. H. Yu, *Angew. Chem. Int. Ed.*, 2014, **53**, 11552-11556.
29. H. Jiang, D. Ren, H. Wang, Y. Hu, S. Guo, H. Yuan, P. Hu, L. Zhang and C. Li, *Adv. Mater.*, 2015, DOI: 10.1002/adma.201501059.
30. S. K. Das, *Mater. Lett.*, 2014, **130**, 240-244.
31. V. O. Koroteev, L. G. Bulusheva, I. P. Asanov, E. V. Shlyakhova, D. V. Vyalikh and A. V. Okotrub, *J. Phys. Chem. C.*, 2011, **115**, 21199-21204.
32. X. Xiao, T. Li, P. Yang, Y. Gao, H. Jin, W. Ni, W. Zhan, X. Zhang, Y. Cao and J. Zhong, *ACS Nano*, 2012, **6**, 9200-9206.
33. P. Yang, X. Xiao, Y. Li, Y. Ding, P. Qiang, X. Tan, W. Mai, Z. Lin, W. Wu and T. Li, *ACS Nano*, 2013, **7**, 2617-2626.
34. J. Z. Wang, L. Lu, M. Lotya, J. N. Coleman, S. L. Chou, H. K. Liu, A. I. Minett and J. Chen, *Adv. Energy Mater.*, 2013, **3**, 798-805.
35. Y. Shi, Y. Wang, J. I. Wong, A. Y. S. Tan, C.-L. Hsu, L.-J. Li, Y.-C. Lu and H. Y. Yang, *Sci. Rep.*, 2013, **3**, 2169.
36. H. Li, X. Wang, B. Ding, G. Pang, P. Nie, L. Shen and X. Zhang, *ChemElectroChem*, 2014, **1**, 1118-1125.
37. Y. Luo, Z. Gong, M. He, X. Wang, Z. Tang and H. Chen, *Sol. Energy Mater. Sol. Cells*, 2012, **97**, 78-82.
38. P. p. Wang, H. Sun, Y. Ji, W. Li and X. Wang, *Adv. Mater.*, 2014, **26**, 964-969.
39. Q. Wang and J. Li, *J. Phys. Chem. C*, 2007, **111**, 1675-1682.
40. H. Li, Q. Zhang, C. C. R. Yap, B. K. Tay, T. H. T. Edwin, A. Olivier and D. Baillargeat, *Adv. Funct. Mater.*, 2012, **22**, 1385-1390.

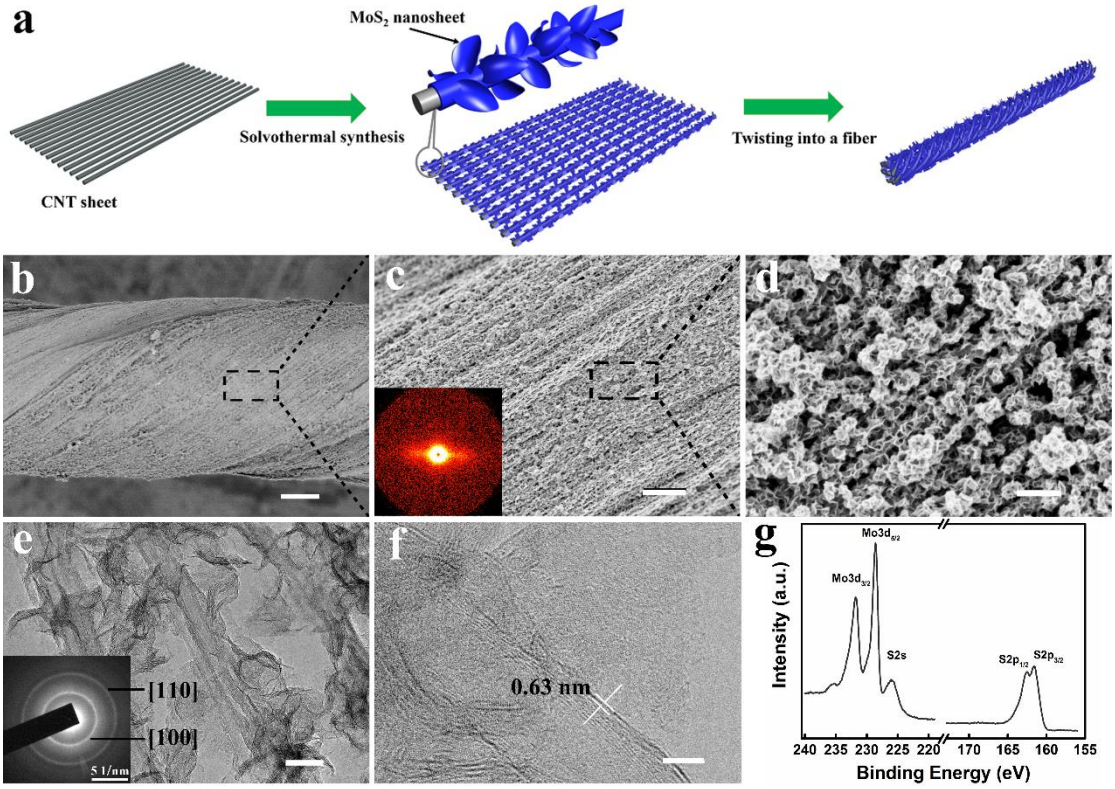

Fig. 1 (a) Schematic illustration to the synthesis of the aligned CNT/MoS_2 hybrid fiber; (b-d) SEM images of a hybrid fiber with increasing magnifications; The inserted image at (c) is the corresponding small angle X-ray scattering pattern; (e) TEM image of CNTs coated with MoS_2 nanosheets with an inserted electron diffraction pattern; (f) Higher magnification of f. (g) X-ray photoelectron spectroscopy spectrum of the aligned CNT/MoS_2 hybrid fiber. Scale bars, 15 μm (b), 2 μm (c), 0.3 μm (d), 30 nm (e) and 5 nm (f).

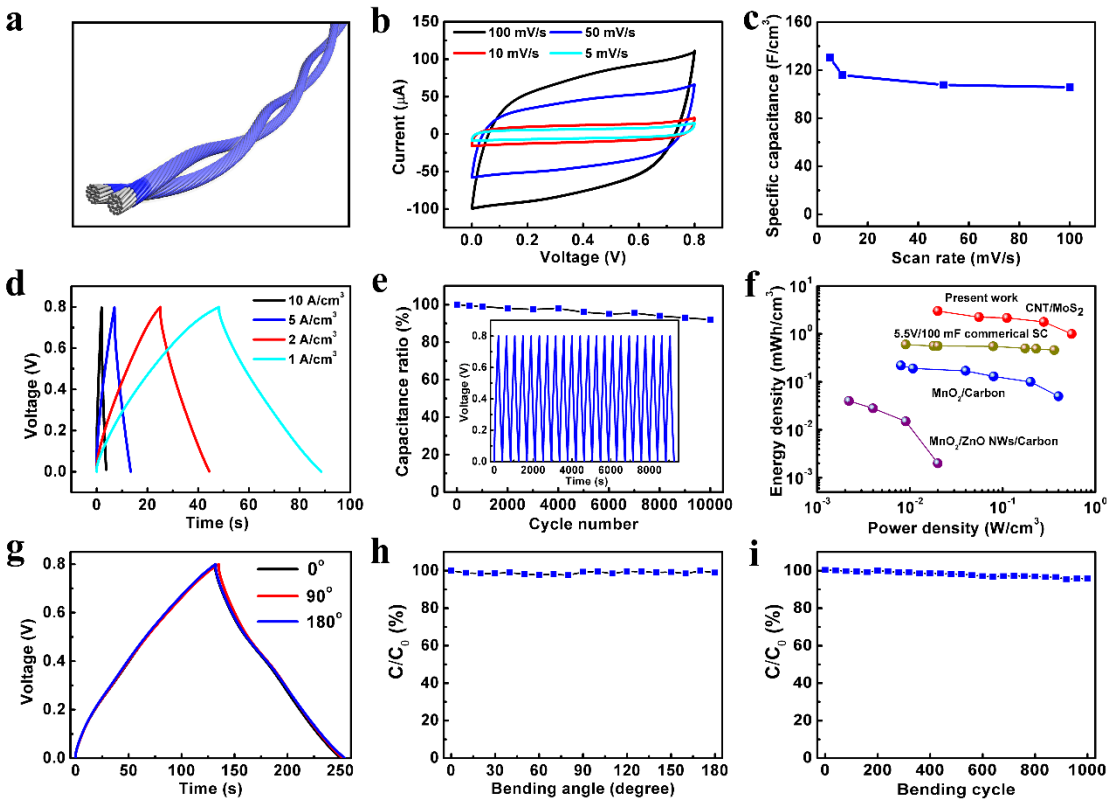

Fig. 2 Electrochemical performances of the fibrous supercapacitor twisted from two aligned CNT/MoS_2 hybrid fibers. (a) Schematic illustration to the structure of the fibrous supercapacitor. (b) Cyclic voltammograms at increasing scan rates. (c) Specific capacitances at increasing scan rates. (d) Galvanostatic charge-discharge profiles at increasing current densities. (e) Cycling performance of the supercapacitor at 1 A cm^{-3} (inserted, charge-discharge profiles). (f) Ragone plots of the present fibrous supercapacitor compared with the commercially available supercapacitor and previous fibrous supercapacitors. (g) Galvanostatic charge-discharge profiles of a fibrous supercapacitor before and after bending by 90° and 180°. (h) Dependence of specific capacitance on bending angle. C_0 and C correspond to the specific capacitances before and after bending to different angles, respectively. (i) Dependence of specific capacitance on bending cycle. C_0 and C correspond to the specific capacitances before and after bending to 90^o for different cycles, respectively.

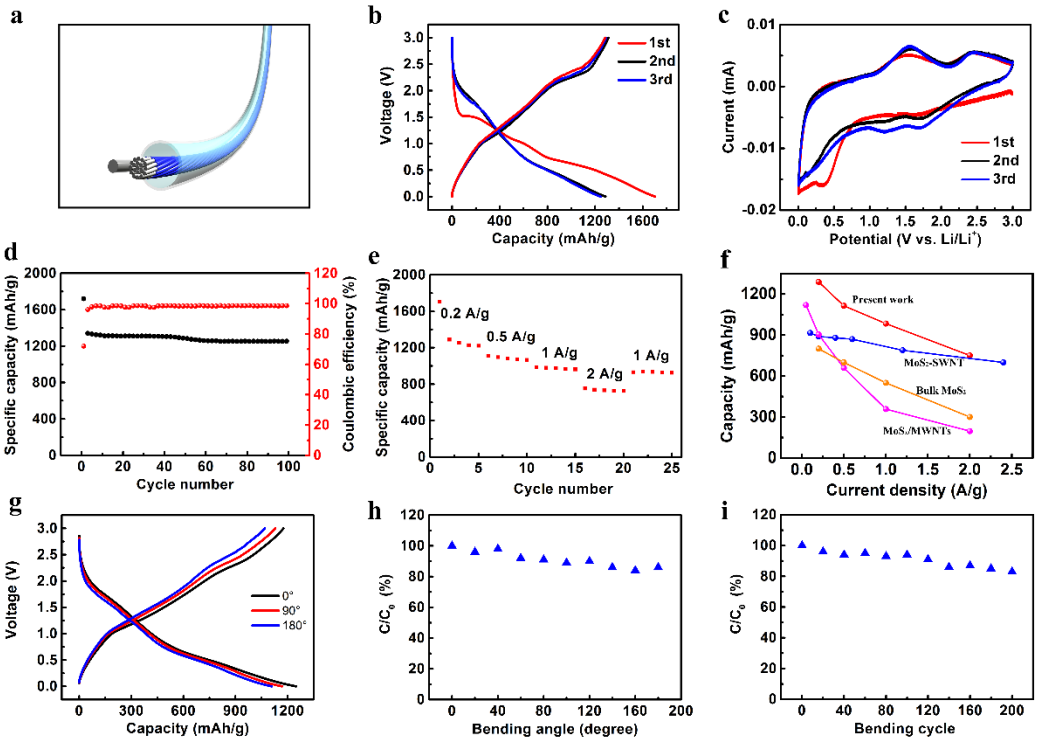

Fig. 3 Electrochemical performances of the fibrous LIB with the aligned CNT/MoS_2 hybrid fiber as the cathode. (a) Schematic illustration to the structure of the fibrous LIB. (b) The first three charge-discharge curves at 0.2 A g^{-1}. c) Cyclic voltammograms at 0.1 mV s^{-1}. (d) Cycling performances at 0.2 A g^{-1}. (e) Rate performances. (f) Specific capacities at increasing current densities compared with previously reported MoS_2-based LIBs. (g) Galvanostatic charge-discharge curves of a fibrous LIB before and after bending by 90° and 180°. (h) Dependence of specific capacity on bending angle. C_0 and C correspond to the specific capacities before and after bending to different angles, respectively. (i) Dependence of specific capacity on bending cycle. C_0 and C correspond to the specific capacities before and after bending to 90° for different cycles, respectively.

The Table of Contents

An aligned carbon nanotube/MoS_2 nanosheet hybrid fiber is synthesized to display combined remarkable mechanical, electronic and electrochemical properties. It is used to fabricate flexible fibrous supercapacitors and lithium ion batteries with high specific capacitance of 135 F cm^{-3} and high specific capacity of 1298 mAh g^{-1}, respectively.